Precision calculation of the 23Ne half-life

Author: Marc Cuevas Torné
*Facultat de Física, Universitat de Barcelona, Diagonal 645, 08028 Barcelona, Spain.**

Advisor: Javier Menéndez Sánchez
(Dated: January 20, 2023)

Abstract: β decay is a common process atomic nuclei go through to end up in a more stable state. In this work I evaluate new nuclear matrix elements in order to obtain a correction to the half-life of the ^{23}Ne β decay. I use the shell model code *Nathan* to evaluate the wave functions of ^{23}Ne and ^{23}Na and the nuclear matrix elements. The new correction reduces the nuclear matrix element of the decay of ^{23}Ne by about 1%. This prediction can be compared with state-of-the-art experiments that search for physics beyond the Standard Model in β decay measurements.

I. INTRODUCTION

The Standard Model is able to describe very accurately a wide range of phenomena, from high-energy collisions in the Large Hadron Collider to nuclear reactions in the core of stars. Although this theory is fairly complete, it is not able to describe some events, including dark matter or the matter antimatter asymmetry of the universe.

Therefore it is important to reanalyze and improve this model. This can be done by several experiments, but in this work we focus on the β decay of ^{23}Ne, which has been recently measured with high precision [1]. This work consists of adding some corrections to the theoretical prediction of the half-life of the nucleus.

A. Beta decay

Beta decay is a radioactive decay that emits either an electron or a positron, for β^- or β^+ decays, correspondingly. In addition, electron capture (EC) is also possible. These processes are summarized as

$$\beta^- : {}^A_Z X \rightarrow {}^A_{Z+1} Y + e^- + \overline{\nu}_e, \tag{1}$$

$$\beta^+ : {}^A_Z X \rightarrow {}^A_{Z-1} Y + e^+ + \nu_e, \tag{2}$$

$$EC : {}^A_Z X + e^- \rightarrow {}^A_{Z-1} Y + \nu_e, \tag{3}$$

where A denotes the sum of protons and neutrons, Z is the number of protons, X and Y are the initial and final atomic nuclei correspondingly. In our case X and Y will be ^{23}Ne and ^{23}Na.

β^- decay is particularly interesting as in the vacuum it releases energy, whereas in β^+ decay and EC the energy release is negative, so energy is needed for them to take place, for instance if the final nucleus is more bound than the initial one. Furthermore there are two types of β decay, the Fermi β decay, in which the spin of the nucleus stays the same, or Gamow-Teller β decay, in which the nucleus spin can change by one unit. Both processes are included in the β decay half-life, which is given by [2]

$$T_{1/2} = \frac{\kappa}{f_0(B_F + B_{GT})}, \tag{4}$$

where $\kappa = 6147s$, f_0 is a phase integral that depends on the type of β decay of interest and lastly B_F and B_{GT} are the reduced transition probabilities for Fermi β decay and Gamow-Teller β decay, respectively

$$B_F = |(f||\hat{C}_0^V(q)||i)|^2, \tag{5}$$

$$B_{GT} = |(f||\hat{L}_1^A(q)||i)|^2, \tag{6}$$

where $|(f||\hat{C}_0^V(q)||i)|$ and $|(f||\hat{L}_1^A(q)||i)|$ are the reduced matrix elements of the operators $\hat{C}_0^V(q)$ and $\hat{L}_1^A(q)$, correspondingly. The initial state $|i\rangle$ is the ^{23}Ne state and the final state $|f\rangle$ is the ^{23}Na final state. These operators are defined by [3]

$$\hat{C}_0^V(q) \simeq \frac{g_V}{2\sqrt{\pi}} \sum_{j=1}^{A} \tau_j^{\pm}, \tag{7}$$

$$\hat{L}_1^A(q) \simeq \frac{i g_A}{2\sqrt{3\pi}} \sum_{j=1}^{A} \vec{\sigma_j} \tau_j^{\pm}, \tag{8}$$

where $g_V = 1$ is the vector coupling constant, $g_A = 1.27$ is the axial vector coupling constant, $\vec{\sigma}$ is the spin operator and $\tau^{\pm}$ is the spin. The summation is for all the nucleons in the nucleus.

B. Shell model

The shell model describes the structure of atomic nucleus thanks to Pauli's exclusion principle. The atomic nucleus is a system of neutrons and protons which interact with each other following two-body interactions described by the Schrödinger's equation

$$\left[\sum_i \frac{-\hbar^2 \nabla_i^2}{2m_i} + \sum_{i<j} V(\vec{r_i}, \vec{r_j})\right] \psi(\vec{r_1}, ..., \vec{r_A}) = E\psi(\vec{r_1}, ..., \vec{r_A}). \tag{9}$$

*Electronic address: mcuevato7@alumnes.ub.edu

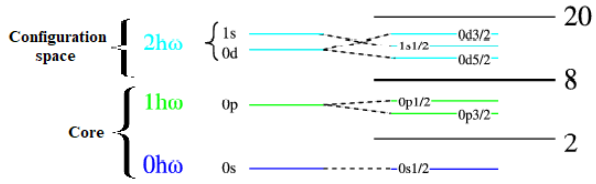

FIG. 1: Harmonic oscillator single-particle levels, extended by the spin-orbit coupling. We distinguish between the core used for the description of the ^{23}Ne and ^{23}Na, ^{16}O, and the configuration space where we will study the different transitions, the *sd* shell. Adapted from [4].

The first term is the kinetic energy, the second one describes the interaction between protons and neutrons in positions $\vec{r_i}$ and $\vec{r_j}$ and E is the total energy for the wave-function ψ. The Hamiltonian can be described in terms of the mean field and a residual interaction between nucleons as

$$H = T + \sum_i v(\vec{r_i}) + V_{RES}. \tag{10}$$

The first two terms can be represented as the harmonic oscillator plus a spin-orbit interaction and compose the mean field approximation, which helps us describe a many-body interaction with a one-body potential. V_{RES} carries all interactions between nucleons. Only when the spin-orbit term is added, one is able to theoretically explain numbers where nuclei becomes very stable. These numbers are called magic numbers.

At first, we use many-body states, which are Slater determinants describing neutrons and protons occupying single-particle states. Figure 1 shows the single-particle basis used to study ^{23}Ne and ^{23}Na. If we analyze more massive nuclei we start having computational problems in consequence of having to calculate an immense number of Slater determinants. Slater determinants are given by

$$\phi(x_1, ..., x_N) = \frac{1}{\sqrt{N!}} \begin{vmatrix} \chi_1(x_1) & \chi_2(x_1) & \cdots & \chi_N(x_1) \\ \chi_1(x_2) & \chi_2(x_2) & \cdots & \chi_N(x_2) \\ \vdots & \vdots & \ddots & \vdots \\ \chi_1(x_N) & \chi_2(x_N) & \cdots & \chi_N(x_N) \end{vmatrix}. \tag{11}$$

In pursuance of calculating larger shells, shell model code *Nathan* [5] takes the low energy nucleons as a core, therefore this core will only need to be represented by a single Slater determinant. The rest of nucleons will be represented by a linear combination of Slater determinants. This simplifies a lot our problem, now the equation to solve is [6]

$$H_{eff} \left|\psi\right\rangle = E \left|\psi\right\rangle, \tag{12}$$

with H_{eff} being the effective Hamiltonian in the valance space. In this work we assume a ^{16}O core, which is doubly-magic nucleus with 8 protons and 8 neutrons. Therefore the valance space will be the *sd* shell, comprising the orbital with $n = 0$ and $l = 2$ and the orbital $n = 1$ and $l = 2$, n being the principal quantum number and l the orbital angular momentum quantum number. Thus the single-particle orbitals for protons and neutrons are $d_{5/2}$, $d_{3/2}$ and $s_{1/2}$. In this work (12) is solved by using the shell-model code *Nathan* [5].

II. ANGULAR MOMENTA AND SPHERICAL TENSORS

To go further in our research we need to define the algebra which is very useful to study nuclear matrix elements such as those of β decay. Starting with angular momenta, for a system of two particles with well defined angular momenta $|j_1, m_1\rangle$ and $|j_2, m_2\rangle$, we define the two-body coupled state to angular momentum j as

$$\begin{aligned} |j_1, j_2; j, m\rangle &= \sum_{m_1, m_2} (j_1, m_1, j_2, m_2 | j, m) \, |j_1, m_1, j_2, m_2\rangle \\ &= \sum_{m_1, m_2} (-1)^{j_1 + j_2 + m} \begin{pmatrix} j_1 & j_2 & j \\ m_1 & m_2 & -m \end{pmatrix} |j_1, m_1, j_2, m_2\rangle, \end{aligned} \tag{13}$$

where $|j_1 - j_2| < j < j_1 + j_2$ is the coupled angular momentum, and $m = m_1 + m_2$ is the projection of the coupled two-body angular momentum. Here $(j_1, m_1, j_2, m_2 | j, m)$ are the Clebsch-Gordan coefficients of this system, which can also be defined as *3j-symbols*, which are the symbols in braces in (13).

When coupling for three angular momenta, the change of uncoupled basis to the coupled basis is given by the *6-j symbols* which appear in braces, [2]

$$\begin{aligned} &|j_1, j_2, j_3(j_{23}); j, m\rangle = \\ &\sum_{j_{12}} (-1)^{j_1 + j_2 + j_3 + j} \hat{j_{12}} \hat{j_{23}} \begin{Bmatrix} j_1 & j_2 & j_{12} \\ j_3 & j & j_{23} \end{Bmatrix} |j_1, j_2, j_3(j_{23}); j, m\rangle. \end{aligned} \tag{14}$$

Here $\hat{j} = \sqrt{2j+1}$. Finally it's also possible to couple four angular momenta but *9-j symbols* are needed, which appear in brackets in (15).

In general, β decay operators can depend on radial and also total angular momentum spaces. In virtue of having each of them act in one space, the operator can be written as the tensor product of two operators, $T_L = [T_{L_1}, T_{L_2}]$ where T_{L_1} and T_{L_2} are two tensors with rank L_1 and L_2 that act on different spaces respectively. Therefore Theorem I from [2] can be used to separate the calculation in the two spaces:

$$\begin{aligned} (n'l' \frac{1}{2} j' || T_L || nl \frac{1}{2} j) &= \hat{j} \hat{j'} \hat{L} \begin{Bmatrix} l' & 1/2 & j' \\ l & 1/2 & j \\ L_1 & L_2 & L \end{Bmatrix} \\ &\cdot (n'l' || T_{L_1} || nl) (\frac{1}{2} || T_{L_2} || \frac{1}{2}). \end{aligned} \tag{15}$$

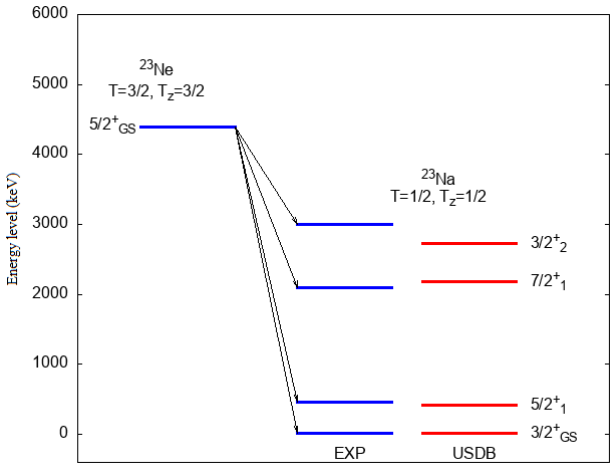

FIG. 2: Decay scheme of ^{23}Ne to ^{23}Na experimental results [8] compared to the ones obtained by using the USDB nuclear Hamiltonian. The experimental and calculated energies show the different states which ^{23}Ne can populate after its β decay.

III. EVALUATION OF NUCLEAR MATRIX ELEMENTS FOR β DECAY

In this work I have implemented a new correction to the β decay, using the shell model code *Nathan*. The β decay that I evaluate is

$$^{23}_{10}Ne \rightarrow ^{23}_{11}Na + e^- + \overline{\nu}_e, \tag{16}$$

where $^{23}_{10}$Ne has total angular momentum and parity $J^P = 5/2^+$. After the decay, $^{23}_{11}$Na has a ground state with $J = 3/2^+$ and three other excited states with $J^P = 3/2^+, 5/2^+$ and $7/2^+$.

To evaluate the β decay operators I calculate the initial and final states for neon and the sodium. To compute this initial and final states I use the Hamiltonian for the USDB interaction [7], which is really accurate for nuclei in the *sd* shell.

There is an experimental energy measured for every transition stated, but I numerically calculate all of them to test the reliability of the calculations. Figure 2 shows the experimental values and the ones calculated using the USDB nuclear Hamiltonian with the shell model code *Nathan*. The transitions to the lowest-energy states ($(\frac{3}{2})^+_{GS}$ and $(\frac{5}{2})^+_1$) have a low discrepancy whereas in transitions to the higher-energy states ($(\frac{7}{2})^+_1$ and $(\frac{3}{2})^+_2$) there is a larger discrepancy of about 200 keV. Finally these energies can be used to compute the different Q_β for each transition.

Recently, Ref.[3] derived an improved expression for the β decay due to Gamow-Teller transitions such as for ^{23}Na:

$$T^{-1}_{1/2} = \frac{f_0}{\kappa} B_{GT}(1 + \delta_{GT}), \tag{17}$$

where δ_{GT} is the correction for the nuclear shape, which should give us a more precise value for the half-life. This shape correction is [3]

$$\delta_{GT} \approx \frac{2}{3}\frac{Q_\beta}{q}\left[\sqrt{2}\frac{|(f||\hat{M}^V_1/q||i)|}{|(f||\hat{L}^A_1||i)|} - \frac{|(f||\hat{C}^A_1/q||i)|}{|(f||\hat{L}^A_1||i)|}\right], \tag{18}$$

with β decay operators [3]:

$$\hat{L}^A_1 = \frac{ig_A}{2\sqrt{3\pi}}\sum_j \vec{\sigma_j}\tau^\pm_j, \tag{19}$$

$$\hat{M}^V_1 = \frac{iq}{2\sqrt{6\pi}m_N}\sum_j [g_V\vec{L_j} + \mu\vec{\sigma_j}]\tau^\pm_j, \tag{20}$$

$$\hat{C}^A_1 = \frac{ig_A q}{2\sqrt{3\pi}m_N}\sum_j [r(\vec{\sigma}\vec{\nabla}) + \frac{1}{2}\vec{\sigma}]\tau^\pm_j. \tag{21}$$

Here $m_N = 939.565$ MeV is the neutron mass, $\mu = 4.7$ is the isovector magnetic moment of the nucleon and q is the transferred linear momentum. $\vec{L}$ is the operator for the orbital angular momentum, and $\vec{r}$ and $\vec{\nabla}$ are the radial and nabla operators. We identify $q \approx Q_\beta$ where

$$\begin{aligned} Q_\beta(f) &= M(^{23}_{10}Ne) - M(^{23}_{11}Na) - M(e^-) = \\ &= m_n - m_p + B(^{23}_{10}Ne) - B(^{23}_{11}Na) - m_e - E_{exc}(f), \end{aligned} \tag{22}$$

where $B(^{23}_{10}Ne)$ and $B(^{23}_{11}Na)$ are the binding energies of Na and Ne nuclei and E_{exc} is the excitation energy of the final states shown in Fig. 2. From [9], $B(^{23}_{10}Ne) = 186.564$ MeV and $B(^{23}_{11}Na) = 182.979$ MeV. Therefore, $Q_\beta(\frac{3}{2}^+_{GS}) = 4.369$ MeV, $Q_\beta(\frac{5}{2}^+_1) = 3.971$ MeV, $Q_\beta(\frac{7}{2}^+_1) = 2.200$ MeV and $Q_\beta(\frac{3}{2}^+_2) = 1.651$ MeV.

The Fermi and Gamow-Teller operators are [2]

$$\begin{aligned} &(l_1, \frac{1}{2}, j_1||\sigma||l_2, \frac{1}{2}, j_2) = \\ &= \sqrt{6}\delta_{l_1,l_2}\hat{j_1}\hat{j_2}(-1)^{3/2+j_1+l_2}\begin{Bmatrix} 1/2 & 1/2 & 1 \\ j_2 & j_1 & l_1 \end{Bmatrix}. \end{aligned} \tag{23}$$

Other operators are needed to evaluate the operators listed in Eqs.(20) and (21). First, we have the angular momentum operator $\vec{L}$, which does not affect the radial part and describes how the angular momentum affects the transition probability. Using (14) we find

$$\begin{aligned} &(l_1, \frac{1}{2}, j_1||L||l_2, \frac{1}{2}, j_2) = \delta_{l_1,l_2}\hat{j_1}\hat{j_2} \\ &\cdot\sqrt{l_1(l_1+1)(2l_1+1)}(-1)^{3/2+j_2+l_2}\begin{Bmatrix} l_1 & l_2 & 1 \\ j_2 & j_1 & 1/2 \end{Bmatrix}. \end{aligned} \tag{24}$$

Secondly, we need to evaluate the $r(\vec{\sigma}\vec{\nabla})$ operator, which operates on the radial part and describes the recoil that the nucleus suffers due to momentum conservation. We

take the results obtained in [8]:

$$(n'l'\frac{1}{2}j'||\vec{r}(\vec{\sigma}\vec{\nabla})||nl\frac{1}{2}j)|_{j=l+\frac{1}{2}} = \sqrt{2}\sqrt{2j'+1}\times$$
$$\left[\delta_{ll'}(l+1)\begin{Bmatrix} l & j' & \frac{1}{2} \\ l+\frac{1}{2} & l+1 & 1\end{Bmatrix}\left(\langle n'l|r\frac{\partial}{\partial r}|nl\rangle - l\delta_{nn'}\right)\right.$$
$$-\delta_{l+2,l'}\sqrt{(l+1)(l+2)}\begin{Bmatrix} l+2 & j' & \frac{1}{2} \\ l+\frac{1}{2} & l+1 & 1\end{Bmatrix}\times$$
$$\left.\left(\langle n'l+2|r\frac{\partial}{\partial r}|nl\rangle - -l\langle n'l+2|nl\rangle\right)\right], \quad (25)$$
$$(n'l'\frac{1}{2}j'||\vec{r}(\vec{\sigma}\vec{\nabla})||nl\frac{1}{2}j)|_{j=l-\frac{1}{2}} = \sqrt{2}\sqrt{2j'+1}\times$$
$$\left[\delta_{ll'}l\begin{Bmatrix} l & j' & \frac{1}{2} \\ l-\frac{1}{2} & l-1 & 1\end{Bmatrix}\left(\langle n'l|r\frac{\partial}{\partial r}|nl\rangle + (l+1)\delta_{nn'}\right)\right.$$
$$-\delta_{l+2,l'}\cdot\sqrt{l(l-1)}\begin{Bmatrix} l-2 & j' & \frac{1}{2} \\ l-\frac{1}{2} & l-1 & 1\end{Bmatrix}\times$$
$$\left.\left(\langle n'l+2|r\frac{\partial}{\partial r}|nl\rangle - -l\langle n'l+2|nl\rangle\right)\right], \quad (26)$$

for two different cases, $j = l - \frac{1}{2}$ and $j = l + \frac{1}{2}$.

Now, I also evaluate the single-particle matrix elements between the basis states in the *sd* shell with their corresponding relative factors in Tables I, II, III, IV and V. I use the code *Nathan* writing a new subroutine for each operator. I did two independent test for Tables II and III, one by directly computing the matrix elements for $[r(\vec{\sigma}\vec{\nabla}) + \frac{1}{2}\vec{\sigma}]$ in the shell code model *Nathan* and secondly computing the matrix elements separately and then adding them up, obtaining the same values.

The first thing to notice is that for the Gamow-Teller and angular momentum operators there are some zeros due to the deltas appearing in Eqs.(23) and (24). In particular for $\vec{L}$ there are zeros alongside the $1s_{1/2}$ column and row as $l = 0$ for the *s* shell. Also, in both operators the non-diagonal elements are antisymmetric.

$\vec{\sigma}$	$0d_{5/2}$	$1s_{1/2}$	$0d_{3/2}$
$0d_{5/2}$	2.89828	0	-3.09839
$1s_{1/2}$	0	2.44949	0
$0d_{3/2}$	3.09839	0	-1.54919

TABLE I: Gamow-Teller operator single-particle matrix elements for the single-particle orbitals of the *sd* shell.

$\vec{L}$	$0d_{5/2}$	$1s_{1/2}$	$0d_{3/2}$
$0d_{5/2}$	5.7966	0	1.5492
$1s_{1/2}$	0	0	0
$0d_{3/2}$	-1.5492	0	4.6476

TABLE II: Same as Table I for the orbital angular momentum operator.

$\vec{r}(\vec{\sigma}\vec{\nabla})$	$0d_{5/2}$	$1s_{1/2}$	$0d_{3/2}$
$0d_{5/2}$	-1.4491	0	-2.3238
$1s_{1/2}$	0	-1,2247	0
$0d_{3/2}$	-5.4222	0	0.7745

TABLE III: Same as Table I for the radial correction to the Gamow-Teller operator.

$g_V\vec{L} + \mu\vec{\sigma}$	$0d_{5/2}$	$1s_{1/2}$	$0d_{3/2}$
$0d_{5/2}$	19.418	0	-13.013
$1s_{1/2}$	0	11.513	0
$0d_{3/2}$	13.013	0	-2.634

TABLE IV: Same as Table I for the reduced matrix elements relevant for the $\hat{M}_1^V$ operator.

$g_A[r(\vec{\sigma}\vec{\nabla}) + \frac{1}{2}\vec{\sigma}]$	$0d_{5/2}$	$1s_{1/2}$	$0d_{3/2}$
$0d_{5/2}$	0	0	-4.91
$1s_{1/2}$	0	0	0
$0d_{3/2}$	-4.91	0	0

TABLE V: Same as Table I for the reduced matrix elements relevant for the $\hat{C}_1^A$ operator.

Comparing the single-particle matrix elements in Tables IV and V we can expect that the $\hat{M}_1^V$ correction is going to be larger than the $\hat{C}_1^A$ correction. Nonetheless we have to calculate the many-body nuclear matrix elements between the initial and final states of the β decay to conclude if it affects the results by much:

$$(f||g_A\vec{\sigma}||i), \quad (27)$$
$$(f||g_V\vec{L} + \mu\vec{\sigma}||i), \quad (28)$$
$$(f||r(\vec{\sigma}\vec{\nabla}) + \frac{1}{2}\vec{\sigma}||i). \quad (29)$$

Transition	$(f\|\|\vec{\sigma}\|\|i)$	$(f\|\|L\|\|i)$	$(f\|\|r(\vec{\sigma}\vec{\nabla})\|\|i)$
$(\frac{5}{2})^+_{GS} \to (\frac{3}{2})^+_{GS}$	0.281	2.54	1.02
$(\frac{5}{2})^+_{GS} \to (\frac{5}{2})^+_1$	0.295	1.93	1.03
$(\frac{5}{2})^+_{GS} \to (\frac{7}{2})^+_1$	0.0922	1.12	0.274
$(\frac{5}{2})^+_{GS} \to (\frac{3}{2})^{+*}_{GS}$	0.219	0.320	0.0995
	$(f\|\|\hat{L}_1^A\|\|i)$	$(f\|\|\frac{\hat{M}_1^V}{\hat{L}_1^A}\|\|i)$	$(f\|\|\frac{\hat{C}_1^A}{\hat{L}_1^A}\|\|i)$
$(\frac{5}{2})^+_{GS} \to (\frac{3}{2})^+_{GS}$	0.0581	0.0356	0.0192
$(\frac{5}{2})^+_{GS} \to (\frac{5}{2})^+_1$	0.0610	0.0265	0.0169
$(\frac{5}{2})^+_{GS} \to (\frac{7}{2})^+_1$	0.0191	0.0220	0.00814
$(\frac{5}{2})^+_{GS} \to (\frac{3}{2})^{+*}_2$	0.0453	0.00603	0.00168

TABLE VI: Value of the many-body nuclear matrix elements for the operators contributing to the ^{23}Ne β decay (results shown with three significant digits).

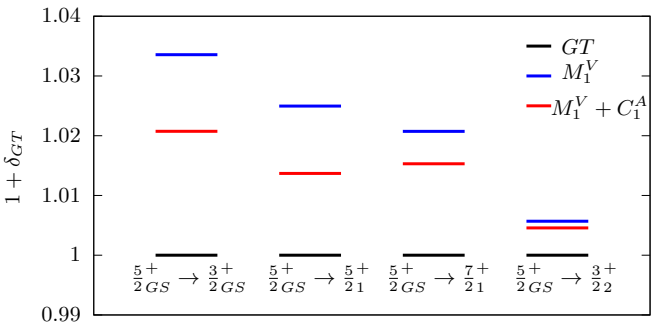

FIG. 3: Modification of the reduced transition probability for the four possible decays of the ^{23}Ne into ^{23}Na. The leading Gamow-Teller result (black) is modified by the correction due to the $\hat{M}_1^V$ (blue) and $\hat{C}_1^A$ operators, which combine to the final result (red).

We now calculate these many-body nuclear matrix elements and we obtain the values shown in Table VI. These results have been tested by exchanging bras and kets, obtaining the same values.

The first term of the correction δ_{GT} in Eq. (18) has been already calculated in Ref.[10]. Table VI collects the results for the many-body nuclear matrix elements entering this correction, proportional to the operator $\hat{M}_1^V$. They reproduce the results found in Ref.[10]. In addition, Table VI also lists the nuclear matrix elements of the second correction of δ_{GT}, corresponding to the operator $\hat{C}_1^A$. These results have been obtained for the first time in this work. Table VI indicates that for the four possible beta decays the contribution from the M_1^V operator is larger than the one from the $\hat{C}_1^A$ operator, typically by a factor 2 or so.

Figure 3 compares the original Gamow-Teller contribution to the decay of ^{23}Ne with the corrections due to δ_{GT}. Firstly, in black we see the result of the leading Gamow-Teller result. Secondly, in blue we see the result if we do not add the correction due to the $\hat{C}_1^A$ operator evaluated in this work. In this case δ_{GT} varies as much as the 2% over the transitions, we obtain 1.033 for the $(\frac{5}{2})^+_{GS} \to (\frac{3}{2})^+_{GS}$ transition and 1.005 for the $(\frac{5}{2})^+_{GS} \to (\frac{3}{2})^{+*}_2$ transition.

Finally, if we add the last term, red lines in Fig. 3, the values for all transitions become closer to 1. This is because the correction from $\hat{C}_1^A$ term enters δ_{GT} with a negative sign, see Eq. (18). In this case the value of δ_{GT} for the $(\frac{5}{2})^+_{GS} \to (\frac{5}{2})^+_1$ transition is smaller than the one for the $(\frac{5}{2})^+_{GS} \to (\frac{7}{2})^+_1$ one. The difference between adding the last correction and not doing it is of the order of 1%, with a maximum of 1.28% for the $(\frac{5}{2})^+_{GS} \to (\frac{3}{2})^+_{GS}$ transition and a minimum of 0.30% for the $(\frac{5}{2})^+_{GS} \to (\frac{3}{2})^+_2$ one.

IV. CONCLUSIONS

To summarise my work I have calculated new matrix elements that are involved in the half-life of the ^{23}Ne β decay. We can see in Eq. (18) two terms, the first one was calculated in Ref.[10] whereas the second term has been calculated for the first time in this work. Reference [10] assumed that the contribution from the $\hat{C}_1^A$ operator, calculated for the first time in this work, was smaller than the $\hat{M}_1^V$ contribution. However, this work shows that the $\hat{C}_1^A$ contribution is roughly a factor two smaller than the $\hat{M}_1^V$ correction.

Taking into account the $\hat{C}_1^A$ operator the decay half-life becomes smaller by 1%. If future experimental measurements of the ^{23}Ne half-life have a 1% precision, my results should be taken into account in the comparison of experimental data with theoretical calculations.

Acknowledgements

I want to acknowledge the help and guidance provided by my advisor Javier Menéndez, who helped me over all difficulties and pushed me throw the rough moments of this work. Also I want to thank my family and friends for being there through all this process.

[1] Y. Mishnayot et al. (2021) arXiv:2107.14355 [nucl-ex].
[2] J. Suhonen, (2007). Springer, Jyväskylä, Finland.
[3] A. Glick-Magid & D.Gazit, (2022). J. Phys. G: Nucl. Part. Phys. Vol. 49, 105105.
[4] https://oer.physics.manchester.ac.uk /NP/Notes/Notes/Notesse23.xht
[5] E. Caurier et al., (2005). Reviews on Modern Physics, Vol. 77, 427-445.
[6] A. Proves & F. Nowacki, (2001). Springer-Verlag. 70-86.
[7] W.A. Richter, S. Mkhize B. A. Brown, (2008). Physical Review C, Vol. 78, 064302.
[8] https://www.nndc.bnl.gov/ensdf/
[9] M. Rovira. Treball Final de Grau, Juny 2022. http://hdl.handle.net/2445/188956.
[10] M. Carrera. Treball Final de Grau, Juny 2021. http://hdl.handle.net/2445/180722.
[11] T.W. Donelly & W.C. Haxton,(1979). Atomic Data and Nuclear Data Tables Vol. 23, 103- 179.